(5) (a) B. D. Vineyard, W. S. Knowles, M. J. Sabacky, G. L. Bachman, and D. J. Weinkauff, *J. Am. Chem. Soc.*, **99**, 5946 (1977); (b) M. D. Fryzuk and B. Bosnick, *ibid.*, **99**, 6262 (1977).
(6) M. A. Bennett and R. Watt, *Chem. Commun.*, 94 (1971).
(7) (a) M. A. Bennett, G. J. Erskine, and R. S. Nyholm, *J. Chem. Soc. A*, 1260 (1967); (b) M. A. Bennett, W. R. Kneen, and R. S. Nyholm, *J. Organomet. Chem.*, **26**, 293 (1971).
(8) P. R. Brookes and R. S. Nyholm, *Chem. Commun.*, 169 (1970).
(9) M. A. Bennett, R. N. Johnson, and I. B. Tomkins, *J. Am. Chem. Soc.*, **96**, 61 (1974).
(10) K. D. Tau, Ph.D. Dissertation, The Ohio State University, March 1978.
(11) (a) D. F. Shriver, "The Manipulation of Air-sensitive Compounds", McGraw-Hill, New York, N.Y., 1969; (b) C. F. Lane and G. W. Kramer, *Aldrichimica Acta*, **10**, 11 (1977).
(12) See, for example, M. Cowie, B. L. Haymore, and J. A. Ibers, *J. Am. Chem. Soc.*, **98**, 7608 (1976).
(13) Supplementary material.
(14) In determining the number of members in the chelate ring, the bonding site of the olefin group is taken as the midpoint of the C=C bond; therefore, the chelate ring is considered intermediate between 5 and 6 members, i.e., 5.5.
(15) P. E. Garrou, *Inorg. Chem.* **14**, 1435 (1975); P. E. Garrou, J. L. S. Curtis, and G. E. Hartwell, *ibid.*, **15**, 3094 (1976).
(16) P. R. Blum, Ph.D. Dissertation, The Ohio State University, Dec 1977.
(17) M. A. Bennett, R. N. Johnson, and I. B. Tomkins, *J. Organomet. Chem.*, **118**, 205 (1976).
(18) S. D. Ittel and J. A. Ibers, *Adv. Organomet. Chem.*, **14**, 33 (1976).
(19) M. J. Bennett and P. B. Donaldson, *Inorg. Chem.*, **16**, 655 (1977).
(20) P. B. Hitchcock, M. McPartlin, and R. Mason, *Chem. Commun.*, 1367 (1969).
(21) D. R. Russell, P. A. Tucker, and S. Wilson, *J. Organomet. Chem.*, **104**, 387 (1976).
(22) H. C. Allen and E. K. Plyler, *J. Am. Chem. Soc.*, **80**, 2673 (1958).
(23) C. A. Tolman, P. Z. Meakin, D. L. Lindner, and J. P. Jesson, *J. Am. Chem. Soc.*, **96**, 2762 (1974).
(24) M. A. Bennett, P. W. Clark, G. B. Robertson, and P. O. Whimp, *J. Chem. Soc., Chem. Commun.*, 1011 (1972).

Contribution from the Department of Chemistry, West Virginia University, Morgantown, West Virginia 26506, the Department of Chemistry, University of Wisconsin—Madison, Madison, Wisconsin 53706, and the Chemistry Division, Argonne National Laboratory, Argonne, Illinois 60439

A Comparison of Room-Temperature Single-Crystal Neutron and X-ray Diffraction Studies of the Bis(triphenylphosphine)iminium Salt of the $[Cr_2(CO)_{10}(\mu\text{-}H)]^-$ Monoanion[1]

JEFFREY L. PETERSEN,*[2a] PAUL L. JOHNSON,[2b] JIM O'CONNOR,[2c] LAWRENCE F. DAHL,*[2c] and JACK M. WILLIAMS*[2b]

Received May 3, 1978

A combined room-temperature X-ray and neutron diffraction study of the bis(triphenylphosphine)iminium salt of the $[Cr_2(CO)_{10}(\mu\text{-}H)]^-$ monoanion has been performed to investigate the effects of crystal packing on the anion and Cr–H–Cr geometry. A comparison with the earlier work on the $[Et_4N]^+$ salt has shown that the pseudo-D_{4h} geometry of the anion's nonhydrogen framework is maintained. This result indicates that the $[Cr_2(CO)_{10}(\mu\text{-}H)]^-$ anion is considerably less susceptible than the tungsten analogue to a twisting deformation from a linear, eclipsed to a bent, staggered configuration. $[(Ph_3P)_2N]^+[Cr_2(CO)_{10}(\mu\text{-}H)]^-$ crystallizes with four molecules in a monoclinic unit cell of symmetry $C2/c$ with X-ray-determined lattice parameters of a = 21.377 (6) Å, b = 16.285 (4) Å, c = 16.186 (5) Å, and β = 128.68 (2)°. The $[(Ph_3P)_2N]^+$ cation lies along the twofold rotation axis which bisects the P–N–P bond angle of 154.8 (4)°; the $[Cr_2(CO)_{10}(\mu\text{-}H)]^-$ anion resides on the crystallographic center of symmetry. Only one position for the bridging hydrogen atom was resolved from the neutron diffraction data with the corresponding maximum negative nuclear density at the center of symmetry. However, the highly anisotropic character of its thermal ellipsoid strongly favors our interpretation that the observed anion structure is consistent with the slightly bent $[Cr_2(CO)_{10}(\mu\text{-}H)]^-$ anion of C_{2v}-$2mm$ geometry (previously observed for the $[Et_4N]^+$ salt) being disordered among four equivalent sites and with the off-axis placement of the bridging hydrogen atom.

Introduction

Our recent neutron diffraction analysis[3] of the tetraethylammonium salt of the $[Cr_2(CO)_{10}(\mu\text{-}H)]^-$ monoanion revealed that the Cr–H–Cr bond is slightly bent (viz. 158.9 (6)°) rather than linear as presumed from earlier single-crystal X-ray diffraction studies.[4] This raised the immediate question regarding the degree to which crystal packing forces influence the Cr–H–Cr geometry. For the tungsten analogue of the monoanion, Bau and co-workers[5] found that the cation can have an appreciable effect on the geometry of the W–H–W bond. For the tetraethylammonium salt a linear, eclipsed metal carbonyl structure exists, whereas for the bis(triphenylphosphine)iminium salt a bent, staggered carbonyl configuration is observed with the W–W separation being 0.11 Å less in the bent form. To investigate the combined influence of packing forces and the cation on the solid-state structure of the Cr–H–Cr bond, we have performed an X-ray and neutron diffraction study at room temperature of the bis(triphenylphosphine)iminium salt of the $[Cr_2(CO)_{10}(\mu\text{-}H)]^-$ monoanion. Substitution of the much larger $[(Ph_3P)_2N]^+$ cation for the $[Et_4N]^+$ one is expected to produce an appreciable change in the molecular packing.

Experimental Section

Crystal Preparation. Suitable crystals of $[(Ph_3P)_2N]^+[Cr_2(CO)_{10}(\mu\text{-}H)]^-$ were grown from saturated and degassed ethanol solutions by slow evaporation in a N_2-filled desiccator which contained magnesium perchlorate. The bis(triphenylphosphine)iminium salt was prepared by published methods.[4,6] Samples of $[(Ph_3P)_2N]^+[Cr_2(CO)_{10}(\mu\text{-}H)]^-$ were kindly supplied by T. Hall of Dr. J. K. Ruff's research group (University of Georgia, Athens, Ga.).

Unit Cell and Space Group. The lattice parameters for $[(Ph_3P)_2N]^+[Cr_2(CO)_{10}(\mu\text{-}H)]^-$ were determined with a Syntex $P\bar{1}$ diffractometer. A triclinic cell with measured lattice constants of a = 13.429 (6) Å, b = 15.040 (6) Å, c = 13.445 (5) Å, α = 107.34 (6)°, β = 105.40 (6)°, γ = 110.97 (5)°, and V = 2199 Å^3 was originally used to collect the X-ray data. However, using the program TRACER II,[7] we later found that the conventional reduced cell is monoclinic. This result was verified via axial X-ray photographs and by a preliminary survey of neutron diffraction reflection intensities. The systematic absences for $\{hkl\}$ of $h + k = 2n + 1$ and for $\{h0l\}$ of $l = 2n + 1$ suggest two possible space groups, Cc (C_s^4, No. 9) and $C2/c$ (C_{2h}^6, No. 15). The centrosymmetric space group $C2/c$ was confirmed from the structure determined. Least-squares fits of the orientation angles 2θ, ω, χ, and ϕ for 15 automatically centered

0020-1669/78/1317-3460$01.00/0

Table I. Crystal Data for $[(Ph_3P)_2N]^+[Cr_2(CO)_{10}(\mu\text{-H})]^-$

	neutron	X-ray
a, Å	21.527 (54)	21.377 (6)
b, Å	16.313 (41)	16.285 (4)
c, Å	16.336 (41)	16.186 (5)
β, deg	128.95 (10)	128.68 (2)
V, Å^3	4461.4	4398.8
μ, cm^{-1}	1.31 (for λ 1.142 Å)	6.498 (for Mo Kα radiation)
space group		$C2/c$ (C_{2h}^6, No. 15)
density, g/cm^3		1.39 (calcd)
		1.39 (measd)
Z		4
formula weight, g/mol		923.7

reflections measured with Mo Kα radiation (λ 0.710 69 Å) or 17 automatically centered reflections ranging in 2θ from 45 to 55° with a neutron wavelength of 1.142 (1) Å produced the lattice constants for $[(Ph_3P)_2N]^+[Cr_2(CO)_{10}(\mu\text{-H})]^-$ at 22 ± 2 °C, which are given in Table I in addition to other pertinent crystal data.

X-ray Data Collection and Structure Analysis. A yellow crystal of dimensions 0.6 × 0.17 × 0.3 mm was mounted under an Ar atmosphere in a thin-walled Lindemann glass capillary. The crystal was transferred to the Syntex diffractometer equipped with a scintillation counter, a pulse-height analyzer adjusted to admit 90% of the Mo Kα peak (λ_{α_1} 0.709 30 Å; λ_{α_2} 0.713 59 Å), and a crystal graphite monochromator set at a Bragg 2θ angle of 12.16°. As indicated previously, the intensity data were measured with diffractometer angles calculated on the basis of a triclinic cell. The θ–2θ scan technique was employed with stationary crystal, stationary counter background counting at each end of a scan. Variable 2θ scan speeds between 2.00 and 24.00°/min and variable scan widths based on the overall intensity and width of the peak were used. Two standard reflections were measured every 48 reflections, and the ratio of total background counting time to scan time was 0.67. No significant changes in the intensities of these monitored reflections were observed during the entire data collection. The triclinic data were sampled once in octants hkl, $\bar{h}kl$, $h\bar{k}l$, $\bar{h}\bar{k}l$ for 3.0° < 2θ < 45.0°. After correction of the intensities for background and polarization of the incident beam due to the crystal monochromator,[8-10] the 6016 data were merged to yield 3266 reflections with $I \geq 2.0\sigma(I)$.[11] A standard deviation, $\sigma(I)$, was estimated for each reflection from the expression

$$\sigma(I) = [(S + B(t_s/t_b)^2)(SR) + 0.05I^2]^{1/2}$$

where S designates the integrated scan count obtained in time t_s, B is the total background count obtained in time t_b, SR is the selected scan rate, and I is the integrated intensity equal to $(S - B(t_s/t_b))(SR)$. An absorption correction was applied[12,13] with resulting transmission coefficients ranging between 0.827 and 0.904.[14]

The reflection data were transformed from the triclinic indexing (hkl) to the monoclinic cell ($h'k'l'$) via the transformation

$$\begin{pmatrix} h' \\ k' \\ l' \end{pmatrix} = \begin{pmatrix} 1 & 0 & -1 \\ -1 & 0 & -1 \\ 0 & 1 & 1 \end{pmatrix} \begin{pmatrix} h \\ k \\ l \end{pmatrix}$$

to yield 1594 independent reflections with $I \geq 2.0\sigma(I)$. The application of heavy-atom methods[15] to a computed three-dimensional Patterson map[16] revealed the initial position for the one independent chromium atom. Successive Fourier syntheses established the coordinates of all remaining nonhydrogen atoms. The initial refinements were performed by block-diagonal least-squares methods.[17] Idealized positions for all of the hydrogen atoms were calculated with MIRAGE,[18] and the refinement was continued with anomalous dispersion corrections included for the Cr and P atoms.[19-22] A full-matrix least-squares refinement[23] with anisotropic temperature factors for all nonhydrogen atoms and with fixed atom contributions from the hydrogen atoms was then carried out. Upon convergence, the final discrepancy values[24] for the 1594 independent reflections were $R(F_o)$ = 0.055 and $R_w(F_o)$ = 0.060. A three-dimensional difference Fourier map revealed no abnormal features with all residual peaks less than 0.6 e/Å^3.

Neutron Data Collection and Structure Analysis. A crystal of approximate dimensions 4.15 mm × 2.05 mm × 2.05 mm and of weight 22.2 mg was sealed in a lead-glass capillary to protect it from moisture and air during data collection. The crystal was mounted in a general orientation on an Electronics and Alloy four-circle diffractometer at the CP-5 research reactor at Argonne National Laboratory. This fully automated diffractometer is operated under the remote control of the Chemistry Division Sigma V computer.[25] A monochromatic neutron beam produced by reflection from the (110) plane of a Be crystal at a monochromator angle of θ_m = 30° was used with a flux of ~2.9 × 10^6 N cm^{-2} s^{-1}. Calibration of the neutron wavelength was made with two standard cubic crystals: NaCl (a = 5.6397 Å) and Si (a = 5.4308 Å) at 22 ± 2 °C.

Table II. Intensity Statistics for $[(Ph_3P)_2N]^+[Cr_2(CO)_{10}(\mu\text{-H})]^-$

	experimental value	theoretical value: centrosymmetric	theoretical value: noncentrosymmetric
E^2	0.9998	1.0000	1.0000
MOD ($E^2 - 1$)	0.9888	0.9680	0.7360
MOD (E)	0.7764	0.7980	0.8860

A θ–2θ step-scan procedure was utilized to collect the neutron intensities of reflections out to (sin θ/λ) = 0.502 with 0.1° step intervals. At each extremity of a scan, a background intensity measurement was made with the crystal and counter being stationary. A total of 2688 reflections were collected. Of the 2464 independent reflections, 107 $h0l$ reflections with $l = 2n + 1$ were systematically absent due to the presence of a c-glide plane in the b direction. Of the remaining 2357 reflections in the data set, 1665 have intensities with $F_o^2 \geq 1.0\sigma(F_o^2)$. Data collection beyond 2θ = 70° was terminated due to the broad and weak nature of the measured diffraction peaks; this was attributed at least in part to large nuclear thermal motion, a relatively high percentage of hydrogen in the crystal, and the mosaic spread of the sample. The combined intensity of two standard reflections, measured after every 80 regular reflections, showed no variations greater than 4%.

The intensities were corrected for Lorentz and absorption (μ_c = 1.31 cm^{-1}, with an incoherent scattering cross-section for hydrogen of 38 barns at λ 1.142 Å) effects. The transmission coefficients ranged from 0.60 to 0.78. The magnitudes of F_o^2 were obtained from the corrected intensities by application of the following equation:[26] $F_o^2 = (\omega I \sin 2\theta)/I_0\lambda^3N^2V$, where I_0 is the incident intensity, λ the wavelength, ω the angular velocity of the crystal, N the number of unit cells per unit volume, V the specimen volume, and θ the Bragg angle. A cylindrical NaCl crystal, for which precise absorption and secondary extinction corrections had been made, was used to obtain I_0 and thereby place the F_o^2 on an approximate "absolute" scale. The variances of F_o^2 were calculated from $\sigma^2(F_o^2) = \sigma_c^2(F_o^2) + (0.05F_o^2)^2$, where $\sigma_c^2(F_o^2)$ is determined from the counting statistics and 0.05 is an empirical factor utilized to account for systematic error.

At the time the neutron diffraction structural analysis was begun, the positions of the nonhydrogen atoms in the salt had not been established by the X-ray diffraction analysis for the monoclinic cell. Based upon the statistical data given in Table II, the neutron diffraction data were shown to be consistent with the centrosymmetric space group, $C2/c$. The positions of all of the nonhydrogen atoms in the $[(Ph_3P)_2N]^+$ monocation were determined from the neutron data with the program MULTAN. Idealized positions of the phenyl hydrogen atoms were calculated[18] from the coordinates of the ring carbon atoms. A full-matrix least-squares refinement of the positional and isotropic temperature parameters for all of the atoms in the cation led to discrepancy indices[24,27,28] of $R(F_o)$ = 0.51, $R(F_o^2)$ = 0.66, and $R_w(F_o^2)$ = 0.71 for the 2357 reflections. The nonhydrogen atoms in the monoanion were identified from a difference Fourier map, and their approximate positions (with isotropic temperature factors) were then included in a further refinement. From a subsequent difference Fourier synthesis, the largest negative trough (corresponding to the bridging hydrogen atom in the Cr–H–Cr bond) was found near the center of symmetry at x = 0.0093, y = 0.0, and z = 0.0. After unsuccessful attempts to refine the bridging H atom off the center of symmetry, its position was fixed at the $\bar{1}$ site. Due to the large number of parameters (viz., 417) present after anisotropic temperature factors for all of the atoms were included in the refinement, six cycles were computed in which half of the parameters associated with the cation were varied during each cycle along with all the positional and temperature parameters of the anion. To eliminate any possible systematic errors introduced by this procedure, all of the positional

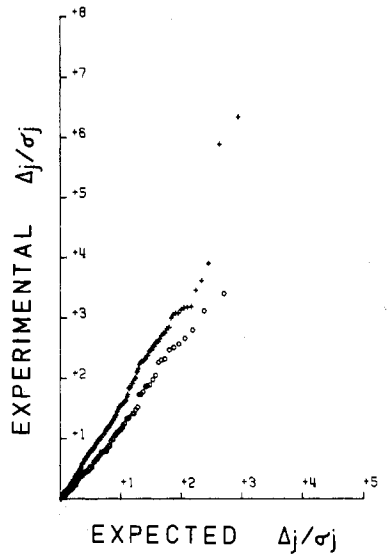

Figure 1. Half-normal probability plot comparing positional (circles) and thermal parameters (crosses) derived from the room-temperature X-ray and neutron diffraction study of $[(Ph_3P)_2N]^+[Cr_2(CO)_{10}(\mu\text{-H})]^-$. Δ_j is equal to $||P_x(j)| - |P_n(j)||$, where $P_x(j)$ and $P_n(j)$ are the final values for parameter j obtained from the X-ray and neutron diffraction data, respectively; σ_j is equal to $\{\sigma^2(P_x(j)) + \sigma^2(P_n(j))\}^{1/2}$, where $\sigma(P_x(j))$ and $\sigma(P_n(j))$ are the corresponding variances in the parameters.

and anisotropic temperature factors for the atoms of the cation were varied simultaneously during two refinement cycles, while the parameters of the monoanion were held constant. Finally, two cycles of full-matrix least-squares refinement on all of the nearly converged parameters led to the discrepancy indices given in Table III. The final scale factor (S) was 0.897 (3); the standard deviation of an observation of unit weight was 0.93 for all 2357 independent reflections. A comparison of the final Fourier and difference Fourier maps based upon the refined structure showed that the largest positive and negative areas on the difference map were only 4 and 11%, respectively, of the corresponding features on the Fourier map. It is noteworthy that a difference map without inclusion of the bridging H atom revealed the largest trough of negative nuclear density to be located exactly on the center of symmetry. No secondary extinction correction appeared to be necessary due to the close agreements between the F_o and F_c for the strong reflections.

Results and Discussion

Comparison of X-ray and Neutron Parameters. The final positional and thermal parameters for the X-ray and neutron diffraction analyses are compared in Table IV. The interatomic distances and bond angles with esd's calculated from the errors in the fractional atomic coordinates are compared wherever possible in Table V. Structure factor tables for both data sets are available.[29] Least-squares planes of interest, calculated from the neutron-determined coordinates, are provided in Table VI.[30,31]

Table III. Final Discrepancy Indices for Structural Analysis of Neutron Diffraction Data

data selection	no. of reflections	$R(F_o)$	$R(F_o^2)$	$R_w(F_o^2)$	σ_1[a]
all data	2357	0.132	0.098	0.106	0.93
reflections with $F_o^2 > 1.0\sigma(F_o^2)$	1665	0.075	0.082	0.098	1.07

[a] σ_1, the standard deviation of an observation of unit weight, is defined by $[\Sigma w_i|F_o^2 - F_c^2|/(n-p)]^{1/2}$ with $w_i^{-1} = \sigma^2(F_o^2) = \sigma_c^2(F_o^2) + (0.05F_o^2)^2$, where σ_c is determined by counting statistics, n is the number of observations, and p is the number of parameters varied (viz., 417) during the least-squares refinement. For appropriately weighted data and normally distributed errors the expected value of σ_1 is unity.

The agreement between the derived parameters from the X-ray and neutron diffraction data was examined by means of a half-normal probability plot[32-34] shown in Figure 1. For the positional parameters of the nonhydrogen atoms (circles in Figure 1) the slope of the half-normal probability plot is essentially linear but slightly larger in magnitude than the ideal value of 1.0 for a normal distribution of errors. This observed deviation indicates that their standard deviations from the least-squares matrix are underestimated by an average factor of 1.2. The plot for the corresponding thermal parameters (crosses in Figure 1) is also linear but with a slightly steeper slope of 1.5. This result is reasonable since one generally expects the thermal parameters to be in poorer agreement than the positional parameters for structural studies of this type. The zero intercept in both plots indicates the absence of any systematic errors associated with the values determined for these parameters.

General Description of the Crystal and Molecular Structure. The crystal structure of $[(Ph_3P)_2N]^+[Cr_2(CO)_{10}(\mu\text{-H})]^-$, as determined from the neutron diffraction data, is depicted stereographically in Figure 2, which shows the arrangement of the four cations and four anions in the centrosymmetric C-centered monoclinic cell. The bis(triphenylphosphine)-iminium cation lies along the twofold rotation axis which bisects the P–N–P bond angle of 154.8 (4)°, whereas the $[Cr_2(CO)_{10}(\mu\text{-H})]^-$ anion lies on a crystallographic center of symmetry. Thus, the crystallographic asymmetric unit contains one independent half-anion and one half-cation with respective site symmetries of C_i-$\bar{1}$ and C_2-2. The closest intermolecular contacts (viz., H(9)···H(9), 2.24 Å; O(1)···H(7), 2.43 Å; O(1)···H(3), 2.48 Å; O(4)···H(6), 2.64 Å; O(2)···H(16), 2.75 Å) do not reflect any unusual interactions among the ions. Figure 2 further shows that the anions occupy channels, which are parallel to the c direction, between the much larger cations in the lattice.

Two different views of the neutron-determined configuration of the $[Cr_2(CO)_{10}(\mu\text{-H})]^-$ monoanion are illustrated in Figure 3. Since the nonhydrogen backbone of the $[Cr_2(CO)_{10}(\mu\text{-H})]^-$

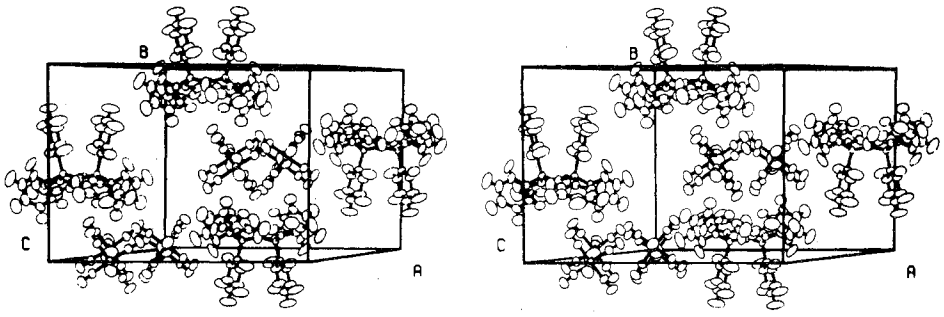

Figure 2. Stereographic view of the arrangement of four $[Cr_2(CO)_{10}(\mu\text{-H})]^-$ anions and four $[(Ph_3P)_2N]^+$ cations in the monoclinic unit cell of symmetry $C2/c$. The thermal ellipsoids of nuclear motion for this and subsequent molecular drawings were scaled to enclose 50% probability.

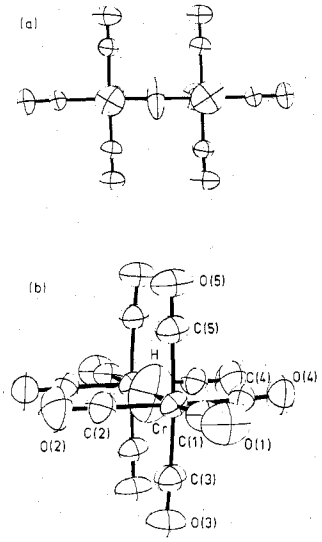

Figure 3. Configuration of the $[Cr_2(CO)_{10}(\mu\text{-H})]^-$ monoanion for the bis(triphenylphosphine)iminium salt showing (a) a view normal to the Cr–Cr axis and (b) a view approximately along the Cr–Cr axis.

anion in the $[(Ph_3P)_2N]^+$ salt is similar to that observed at room temperature for the $[Et_4N]^+$ salt, one must conclude that the pseudo-D_{4h} geometry of the anion's nonhydrogen framework is much less susceptible to deformation by crystal packing effects than that for the tungsten analogue. For the $[W_2(CO)_{10}(\mu\text{-H})]^-$ monoanion in the $[NEt_4]^+$ salt, a linear, eclipsed metal carbonyl configuration is observed, whereas in the $[(Ph_3P)_2N]^+$ salt an appreciably bent, staggered carbonyl structure for the anion is found. In addition, the metal–metal separations in the two tungsten salts differ significantly with the W–W distance being 0.11 Å smaller in the bent configuration.[4,5]

In contrast to the twofold disordered structure previously resolved for the bridging hydrogen atom in $[Et_4N]^+[Cr_2(CO)_{10}(\mu\text{-H})]^-$, only one bridging hydrogen atom position was located in the $[(Ph_3P)_2N]^+$ salt with the maximum negative nuclear density being at the center of symmetry. As illustrated in these two orientations of the anion, the highly anisotropic thermal ellipsoid associated with the bridging hydrogen atom indicates that its equilibrium position is not clearly resolved at room temperature. Although the Cr–H–Cr bond in Figure 3 is depicted as linear, the large amplitudes of the two root-mean-square components of thermal displacement normal to the Cr–Cr vector (i.e., $\mu(2)$ = 0.422 (38) Å and $\mu(3)$ = 0.532 (25) Å) strongly suggest the presence of a disordered hydrogen atom (vide infra).

The essential structural features obtained from our X-ray and neutron diffraction studies of the $[Et_4N]^+$ and $[(Ph_3P)_2N]^+$ salts of the $[Cr_2(CO)_{10}(\mu\text{-H})]^-$ monoanion are compared in Table VI. The observed differences between the neutron-determined values for the Cr–C(1) and C(1)–O(1) distances in the two salts, in light of the X-ray results for the $[(Ph_3P)_2N]^+$ salt, are not significant and to some degree reflect the uncertainty in these parameters. Although the basic nonhydrogen framework of the monoanion in the two salts is similar, the shorter Cr···Cr′ separation in the $[(Ph_3P)_2N]^+$ salt reflects a larger metal–metal bonding component for the Cr–H–Cr bond in this salt.

The structure of the bis(triphenylphosphine)iminium monocation with atom labeling is illustrated stereographically in Figure 4. This cation corresponds to the usual bent P–N–P configuration[35-41] in contrast to the linear structure found by Wilson and Bau[42] for the $[V(CO)_6]^-$ salt. The three independent phenyl rings are each coplanar (see Table VII) within experimental error; a nearly tetrahedral geometry is observed about the independent phosphorus atom.

The Bridging Hydrogen Atom in the $[Cr_2(CO)_{10}(\mu\text{-H})]^-$ Monoanion. Our room-temperature neutron diffraction studies involving two different crystalline environments of the $[Cr_2(CO)_{10}(\mu\text{-H})]^-$ monoanion have established that the bridging hydrogen atom is disposed symmetrically between the two chromium atoms in both cases. In the $[Et_4N]^+$ salt a disordered, slightly bent structure for the Cr–H–Cr bond has been resolved with experimentally equivalent Cr–H in-

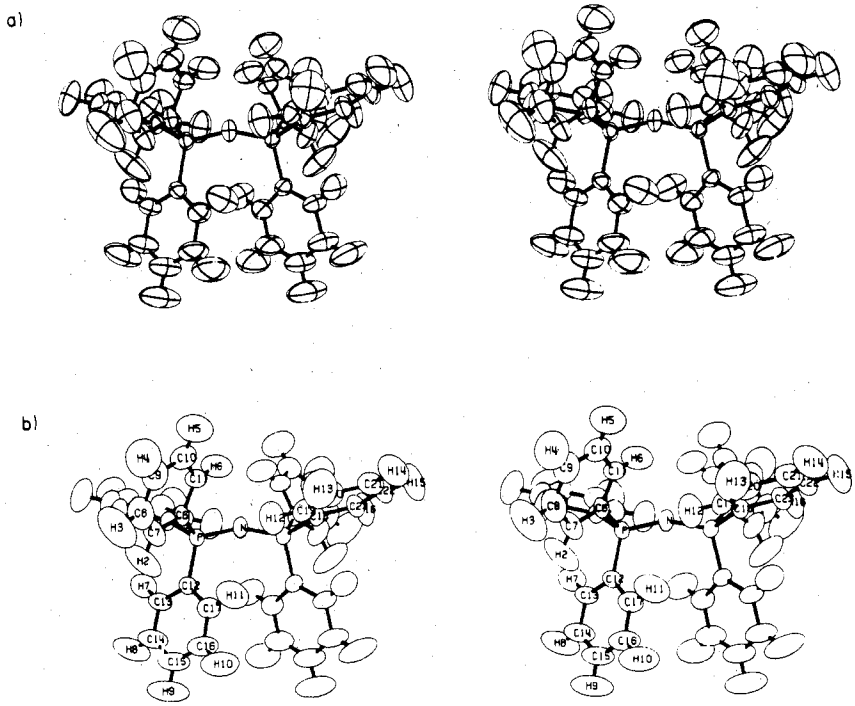

Figure 4. Stereographic drawings of the molecular configuration of the bis(triphenylphosphine)iminium cation showing (a) thermal ellipsoids of nuclear motion and (b) the atom labeling. The anion lies on a crystallographic twofold rotation axis which bisects the P–N–P bond angle of 154.8 (4)°.

Table IV. Positional and Thermal Parameters for $[(Ph_3P)_2N]^+[Cr_2(CO)_{10}(\mu\text{-}H)]^-$ and Root-Mean-Square Thermal Displacements (in Å) of Atoms along Their Principal Ellipsoidal Axes[a-d]

atom	10^4x	10^4y	10^4z	$10^4\beta_{11}$	$10^4\beta_{22}$	$10^4\beta_{33}$	$10^4\beta_{12}$	$10^4\beta_{13}$	$10^4\beta_{23}$	$10^3\mu(1)$	$10^3\mu(2)$	$10^3\mu(3)$
Cr	617 (4)	232 (4)	1284 (5)	27 (3)	43 (3)	40 (5)	0 (2)	19 (3)	2 (3)	180 (11)	203 (24)	241 (10)
	626 (1)	235 (1)	1294 (1)	37 (1)	44 (1)	55 (1)	0 (1)	28 (1)	0 (1)			
C(1)	1305 (3)	437 (3)	2726 (4)	35 (2)	57 (2)	46 (4)	5 (2)	16 (2)	−6 (2)	187 (6)	239 (12)	303 (9)
	1291 (4)	439 (4)	2702 (6)	40 (3)	52 (5)	76 (7)	7 (3)	30 (4)	−3 (4)			
O(1)	1736 (4)	569 (4)	3606 (5)	54 (3)	86 (4)	55 (5)	6 (3)	19 (3)	−10 (3)	205 (8)	307 (13)	372 (11)
	1731 (3)	575 (4)	3607 (4)	54 (3)	80 (4)	66 (5)	7 (3)	23 (3)	−7 (3)			
C(2)	1020 (3)	1159 (3)	1047 (4)	40 (2)	44 (2)	88 (4)	−4 (2)	39 (2)	−2 (2)	221 (10)	254 (9)	270 (8)
	1022 (5)	1147 (5)	1052 (6)	47 (4)	47 (5)	90 (8)	5 (3)	43 (5)	1 (4)			
O(2)	1276 (4)	1712 (4)	933 (6)	90 (4)	63 (3)	180 (8)	−22 (3)	94 (5)	−3 (4)	231 (22)	351 (20)	390 (6)
	1277 (4)	1706 (4)	932 (5)	96 (4)	61 (4)	166 (7)	−20 (3)	93 (5)	−6 (5)			
C(3)	−169 (2)	921 (3)	1107 (3)	37 (2)	54 (2)	70 (3)	7 (2)	33 (2)	4 (2)	216 (11)	239 (5)	278 (5)
	−169 (5)	920 (5)	1101 (6)	52 (4)	50 (5)	80 (7)	0 (4)	43 (5)	8 (4)			
O(3)	−623 (4)	1367 (4)	1006 (5)	60 (3)	75 (4)	139 (7)	21 (3)	63 (4)	10 (4)	232 (19)	331 (15)	352 (6)
	−618 (4)	1364 (4)	1012 (5)	64 (3)	69 (4)	157 (7)	20 (3)	72 (4)	12 (4)			
C(4)	205 (3)	−707 (3)	1473 (3)	43 (2)	48 (2)	68 (3)	0 (2)	35 (2)	9 (2)	213 (14)	248 (6)	268 (8)
	206 (4)	−701 (6)	1478 (6)	52 (4)	50 (5)	75 (7)	2 (3)	44 (5)	−1 (4)			
O(4)	−26 (4)	−1290 (4)	1588 (5)	77 (4)	59 (3)	120 (6)	−7 (3)	68 (4)	13 (3)	226 (21)	325 (9)	336 (10)
	−30 (4)	−1282 (4)	1590 (5)	90 (4)	55 (4)	145 (7)	−13 (3)	85 (5)	2 (3)			
C(5)	1417 (3)	−407 (3)	1427 (3)	37 (2)	52 (2)	75 (4)	3 (2)	32 (2)	0 (2)	225 (10)	249 (9)	269 (8)
	1411 (5)	−409 (5)	1418 (6)	44 (4)	48 (5)	73 (6)	0 (3)	33 (4)	−6 (4)			
O(5)	1906 (4)	−784 (4)	1524 (5)	46 (3)	87 (4)	112 (6)	16 (3)	45 (3)	−6 (4)	220 (18)	300 (9)	371 (10)
	1902 (3)	−785 (4)	1523 (5)	52 (3)	83 (4)	133 (6)	16 (3)	55 (4)	−3 (4)			
H(1)	0	0	0	103 (10)	180 (15)	44 (9)	−41 (12)	23 (9)	−27 (11)	178 (22)	422 (38)	532 (25)
	0	0	0									
N	5000	817 (2)	2500	19 (1)	46 (2)	70 (3)	0	20 (2)	0	161 (8)	250 (5)	262 (10)
	5000	820 (5)	2500	28 (3)	38 (4)	80 (1)	0	31 (4)	0			
P	5857 (2)	607 (3)	2880 (3)	19 (2)	31 (2)	43 (3)	1 (2)	14 (2)	−2 (2)	162 (7)	195 (12)	220 (13)
	5856 (1)	609 (1)	2885 (1)	24 (1)	32 (1)	52 (1)	1 (1)	19 (1)	0 (1)			
C(6)	6005 (2)	1081 (2)	2016 (3)	18 (1)	42 (2)	46 (3)	4 (1)	13 (2)	4 (2)	154 (6)	222 (13)	241 (6)
	6011 (4)	1079 (4)	2029 (5)	28 (3)	38 (4)	45 (5)	0 (3)	17 (3)	−5 (4)			
C(7)	6455 (3)	699 (4)	1779 (4)	46 (2)	72 (3)	82 (4)	23 (2)	45 (3)	23 (3)	206 (17)	234 (11)	343 (6)
	6453 (4)	704 (5)	1782 (6)	46 (4)	56 (5)	83 (7)	17 (3)	39 (5)	18 (5)			
C(8)	6581 (4)	1103 (4)	1137 (4)	61 (3)	100 (4)	99 (5)	17 (3)	63 (3)	27 (4)	204 (29)	281 (6)	388 (7)
	6580 (6)	1104 (7)	1137 (8)	69 (5)	102 (7)	123 (9)	22 (5)	76 (6)	24 (7)			
C(9)	6269 (3)	1876 (4)	751 (5)	54 (3)	87 (4)	84 (4)	1 (3)	48 (3)	24 (3)	211 (22)	278 (6)	361 (8)
	6269 (6)	1872 (7)	757 (7)	60 (5)	77 (6)	83 (7)	4 (4)	48 (5)	24 (5)			
C(10)	5816 (3)	2257 (4)	988 (4)	57 (3)	52 (3)	80 (4)	−5 (2)	45 (3)	9 (3)	212 (18)	273 (5)	301 (11)
	5824 (5)	2246 (5)	992 (6)	63 (5)	42 (4)	86 (7)	0 (4)	46 (5)	13 (5)			
C(11)	5688 (3)	1859 (3)	1619 (3)	38 (2)	32 (2)	67 (3)	2 (2)	29 (2)	7 (2)	198 (8)	234 (5)	252 (16)
	5697 (4)	1852 (5)	1631 (6)	41 (4)	36 (4)	72 (6)	−6 (3)	33 (4)	−3 (4)			
C(12)	6046 (2)	−461 (2)	2920 (3)	27 (2)	31 (2)	51 (3)	4 (1)	17 (2)	2 (2)	181 (5)	209 (6)	245 (15)
	6052 (4)	−466 (4)	2921 (5)	30 (3)	35 (4)	60 (6)	−3 (3)	24 (4)	−3 (4)			
C(13)	6704 (3)	−825 (3)	3834 (4)	48 (2)	32 (2)	66 (4)	8 (2)	33 (3)	9 (2)	193 (8)	239 (11)	274 (12)
	6698 (5)	−827 (4)	3828 (6)	53 (4)	35 (4)	62 (6)	30 (3)	35 (4)	36 (4)			
C(14)	6852 (4)	−1660 (3)	3861 (5)	81 (3)	37 (3)	96 (5)	15 (3)	54 (4)	16 (3)	204 (10)	283 (15)	355 (12)
	6833 (6)	−1660 (5)	3837 (7)	79 (6)	42 (5)	97 (9)	18 (4)	53 (6)	27 (5)			
C(15)	6327 (4)	−2131 (4)	2973 (5)	91 (4)	35 (3)	136 (6)	7 (3)	71 (4)	−3 (4)	210 (10)	330 (13)	364 (13)
	6327 (8)	−2131 (5)	2973 (8)	100 (7)	33 (5)	150 (12)	8 (5)	80 (8)	−5 (6)			
C(16)	5668 (4)	−1772 (3)	2046 (5)	73 (3)	40 (3)	109 (6)	−4 (3)	35 (3)	−30 (3)	185 (13)	306 (6)	405 (17)
	5690 (6)	−1776 (6)	2071 (8)	78 (6)	47 (6)	117 (10)	−7 (5)	45 (6)	−40 (6)			
C(17)	5539 (3)	−948 (3)	2023 (4)	41 (2)	43 (3)	77 (4)	−1 (2)	15 (3)	−25 (3)	177 (9)	246 (7)	364 (13)
	5543 (5)	−944 (6)	2032 (6)	46 (4)	51 (5)	81 (8)	0 (4)	26 (5)	−17 (5)			
C(18)	6589 (2)	1016 (2)	4178 (3)	18 (2)	39 (2)	35 (2)	0 (1)	8 (2)	−2 (2)	148 (5)	222 (12)	231 (8)

	6596 (4)	1018 (4)	4188 (5)	26 (3)	28 (3)	55 (6)	1 (3)	18 (4)	3 (3)			
C(19)	6401 (3)	1113 (3)	4849 (3)	32 (2)	52 (2)	43 (3)	7 (2)	15 (2)	−2 (2)	183 (6)	226 (14)	290 (10)
	6406 (4)	1117 (5)	4850 (6)	36 (4)	58 (5)	64 (7)	2 (3)	27 (4)	−4 (4)			
C(20)	6967 (4)	1420 (3)	5864 (4)	52 (3)	66 (3)	44 (4)	4 (2)	20 (3)	−12 (3)	181 (10)	281 (9)	340 (12)
	6980 (6)	1423 (5)	5859 (6)	57 (5)	56 (5)	54 (6)	6 (4)	29 (5)	−6 (4)			
C(21)	7718 (4)	1621 (3)	6206 (5)	48 (3)	48 (2)	54 (4)	−5 (2)	11 (3)	−9 (2)	186 (8)	261 (6)	353 (17)
	7721 (6)	1618 (5)	6196 (6)	52 (5)	50 (5)	50 (7)	−7 (4)	8 (5)	−7 (4)			
C(22)	7918 (3)	1521 (3)	5551 (4)	27 (2)	62 (3)	61 (4)	−13 (2)	−1 (3)	−5 (3)	146 (9)	288 (7)	358 (14)
	7903 (5)	1528 (5)	5533 (7)	37 (4)	57 (5)	82 (8)	−15 (4)	16 (5)	−4 (5)			
C(23)	7354 (3)	1223 (3)	4525 (4)	26 (2)	50 (2)	68 (4)	−7 (2)	15 (3)	−1 (2)	180 (7)	258 (7)	296 (15)
	7343 (5)	1220 (5)	4522 (6)	37 (4)	49 (4)	70 (7)	−9 (3)	26 (4)	−4 (4)			
H(2)	6709 (8)	100 (9)	2083 (10)	117 (8)	102 (7)	176 (13)	69 (7)	122 (9)	68 (9)	217 (56)	271 (36)	506 (10)
	6694	136	2074									
H(3)	6949 (10)	802 (10)	966 (13)	133 (10)	154 (11)	231 (18)	70 (9)	152 (13)	71 (12)	247 (86)	350 (23)	555 (12)
	6920	827	971									
H(4)	6377 (8)	2190 (9)	251 (11)	99 (8)	132 (10)	161 (13)	12 (7)	97 (9)	55 (9)	243 (57)	367 (16)	466 (15)
	6368	2169	287									
H(5)	5566 (8)	2838 (8)	666 (11)	113 (8)	71 (6)	170 (13)	20 (6)	105 (9)	38 (8)	258 (30)	331 (41)	423 (10)
	5590	2820	707									
H(6)	5336 (7)	2141 (6)	1779 (9)	89 (6)	52 (5)	143 (11)	13 (4)	86 (8)	18 (5)	252 (15)	280 (48)	372 (9)
	5365	2129	1810									
H(7)	7123 (6)	−467 (6)	4537 (8)	52 (4)	63 (5)	54 (7)	10 (4)	8 (5)	4 (5)	191 (11)	288 (13)	378 (23)
	7086	−483	4493									
H(8)	7367 (9)	−1910 (7)	4570 (12)	116 (8)	59 (6)	145 (14)	42 (6)	56 (10)	31 (8)	216 (12)	370 (20)	489 (67)
	7326	−1927	4535									
H(9)	6442 (9)	−2789 (8)	2981 (11)	146 (10)	42 (6)	185 (15)	21 (6)	86 (10)	5 (8)	226 (18)	390 (15)	506 (33)
	6428	−2749	2983									
H(10)	5267 (8)	−2135 (8)	1343 (13)	107 (9)	60 (6)	184 (16)	−3 (6)	35 (10)	−44 (9)	239 (21)	360 (13)	562 (33)
	5288	−2126	1389									
H(11)	5019 (7)	−657 (7)	1290 (9)	68 (5)	76 (6)	80 (9)	15 (5)	−8 (6)	−23 (6)	201 (14)	294 (17)	514 (21)
	5048	−682	1347									
H(12)	5808 (6)	964 (7)	4562 (8)	49 (5)	110 (7)	91 (8)	−11 (5)	45 (6)	−20 (6)	250 (40)	262 (10)	393 (12)
	5842	970	4589									
H(13)	6824 (7)	1500 (9)	6375 (9)	86 (7)	141 (10)	88 (9)	5 (6)	59 (7)	−22 (8)	231 (36)	351 (19)	449 (17)
	6820	1501	6344									
H(14)	8165 (7)	1851 (7)	6988 (9)	65 (5)	89 (7)	77 (9)	−22 (5)	−1 (6)	−27 (7)	177 (17)	364 (12)	469 (24)
	8136	1851	6947									
H(15)	8501 (7)	1682 (8)	5795 (9)	39 (5)	133 (9)	121 (11)	−30 (5)	22 (6)	−19 (8)	202 (17)	387 (27)	442 (16)
	8474	1672	5796									
H(16)	7496 (5)	1166 (8)	4023 (9)	34 (4)	113 (7)	103 (9)	−21 (4)	36 (5)	−20 (7)	199 (20)	302 (26)	402 (12)
	7495	1142	4041									

[a] For each atom, the neutron diffraction result is given on the first line with the corresponding X-ray diffraction result on the line below it. [b] The estimated standard deviations in parentheses for this and all subsequent tables refer to the least significant figure. [c] The form of the anisotropic temperature factor is $\exp\{-(\beta_{11}h^2 + \beta_{22}k^2 + \beta_{33}l^2 + 2\beta_{12}hk + 2\beta_{13}hl + 2\beta_{23}kl)\}$. [d] In the final full-matrix least-squares refinement of the X-ray diffraction data, the positional and isotropic thermal parameters of the hydrogen atoms are assigned as fixed contributors obtained using idealized coordinates. The isotropic temperature factor was arbitrarily assigned a value of $B = 5.0$ Å^2 for all hydrogen atoms.

Table V. Interatomic Distances (Å) and Bond Angles (deg) for $[(Ph_3P)_2N]^+[Cr_2(CO)_{10}(\mu\text{-}H)]^-$ [a,b]

	neutron	X-ray
(A) Distances for the $[Cr_2(CO)_{10}(\mu\text{-}H)]^-$ Monoanion		
Cr-Cr	3.349 (13)	3.359 (2)
Cr-H(1)	1.675	1.679
Cr-C(1)	1.862 (8)	1.817 (8)
Cr-C(2)	1.901 (10)	1.870 (8)
Cr-C(3)	1.895 (9)	1.886 (8)
Cr-C(4)	1.890 (10)	1.886 (8)
Cr-C(5)	1.899 (11)	1.880 (8)
C(1)-O(1)	1.140 (7)	1.159 (7)
C(2)-O(2)	1.133 (11)	1.136 (8)
C(3)-O(3)	1.144 (9)	1.138 (8)
C(4)-O(4)	1.141 (9)	1.138 (8)
C(5)-O(5)	1.139 (10)	1.134 (7)
(B) Distances for the Bis(triphenylphosphine)iminium Cation, $[(Ph_3P)_2N]^+$		
N-P	1.571 (5)	1.553 (2)
P-C(6)	1.805 (8)	1.779 (7)
P-C(12)	1.781 (6)	1.791 (7)
P-C(18)	1.796 (5)	1.793 (7)
av	1.794 (7)	1.788 (4)
Around First Phenyl Ring		
C(6)-C(7)	1.396 (9)	1.373 (9)
C(7)-C(8)	1.402 (12)	1.395 (10)
C(8)-C(9)	1.381 (10)	1.353 (11)
C(9)-C(10)	1.401 (12)	1.366 (10)
C(10)-C(11)	1.384 (10)	1.396 (9)
C(11)-C(6)	1.392 (6)	1.377 (9)
av	1.393 (4)	1.377 (7)
C(7)-H(2)	1.077 (15)	
C(8)-H(3)	1.106 (26)	
C(9)-H(4)	1.105 (22)	
C(10)-H(5)	1.052 (14)	
C(11)-H(6)	1.051 (19)	
av	1.078 (12)	
Around Second Phenyl Ring		
C(12)-C(13)	1.389 (5)	1.372 (9)
C(13)-C(14)	1.394 (7)	1.393 (10)
C(14)-C(15)	1.382 (8)	1.354 (10)
C(15)-C(16)	1.395 (8)	1.356 (11)
C(16)-C(17)	1.367 (8)	1.390 (11)
C(17)-C(12)	1.399 (6)	1.379 (9)
av	1.388 (5)	1.374 (7)
C(13)-H(7)	1.082 (10)	
C(14)-H(8)	1.058 (13)	
C(15)-H(9)	1.110 (14)	
C(16)-H(10)	1.082 (15)	
C(17)-H(11)	1.108 (10)	
av	1.088 (10)	
Around Third Phenyl Ring		
C(18)-C(19)	1.396 (9)	1.367 (9)
C(19)-C(20)	1.394 (6)	1.392 (10)
C(20)-C(21)	1.378 (11)	1.357 (10)
C(21)-C(22)	1.391 (13)	1.351 (10)
C(22)-C(23)	1.401 (7)	1.389 (9)
C(23)-C(18)	1.404 (7)	1.368 (8)
av	1.394 (4)	1.371 (7)
C(19)-H(12)	1.076 (15)	
C(20)-H(13)	1.064 (21)	
C(21)-H(14)	1.073 (12)	
C(22)-H(15)	1.082 (17)	
C(23)-H(16)	1.044 (19)	
av	1.068 (7)	
(C) Bond Angles for the $[Cr_2(CO)_{10}(\mu\text{-}H)]^-$ Monoanion[c]		
Cr-H(1)-Cr′	180	180
H(1)-Cr-C(1)	177.3 (5)	177.1
H(1)-Cr-C(2)	91.6 (4)	91.7
H(1)-Cr-C(3)	90.8 (3)	89.6
H(1)-Cr-C(4)	86.4 (3)	85.7
H(1)-Cr-C(5)	88.5 (4)	87.9
C(1)-Cr-C(2)	90.7 (3)	91.1 (3)
C(1)-Cr-C(3)	90.6 (4)	91.1 (3)
C(1)-Cr-C(4)	91.2 (4)	91.4 (3)
C(1)-Cr-C(5)	90.2 (3)	91.5 (3)
C(2)-Cr-C(3)	88.6 (3)	88.4 (3)
Cr-C(1)-O(1)	178.7 (8)	178.3 (7)
Cr-C(2)-O(2)	178.2 (5)	177.8 (7)
Cr-C(3)-O(3)	176.9 (5)	176.5 (7)
Cr-C(4)-O(4)	177.7 (7)	178.2 (7)
Cr-C(5)-O(5)	179.0 (5)	177.2 (7)
C(2)-Cr-C(4)	177.9 (6)	177.3 (3)
C(2)-Cr-C(5)	88.1 (5)	88.5 (3)
C(3)-Cr-C(4)	89.5 (3)	92.3 (3)
C(3)-Cr-C(5)	176.5 (6)	176.0 (3)
C(4)-Cr-C(5)	88.1 (4)	90.7 (3)
D. Bond Angles for the Bis(triphenylphosphine)iminium Cation, $[(Ph_3P)_2N]^+$		
P-N-P′	154.8 (4)	154.6 (3)
N-P-C(6)	109.7 (3)	109.5 (3)
N-P-C(12)	114.3 (3)	114.8 (4)
N-P-C(18)	109.1 (4)	109.8 (3)
C(6)-P-C(12)	107.4 (4)	107.0 (3)
C(6)-P-C(18)	108.0 (3)	107.4 (3)
C(12)-P-C(18)	108.1 (3)	107.8 (3)
Around First Phenyl Ring		
C(11)-C(6)-C(7)	120.0 (5)	119.5 (7)
C(6)-C(7)-C(8)	119.5 (5)	119.9 (8)
C(7)-C(8)-C(9)	120.2 (8)	120.1 (8)
C(8)-C(9)-C(10)	120.1 (8)	120.7 (8)
C(9)-C(10)-C(11)	119.8 (5)	119.6 (8)
C(10)-C(11)-C(6)	120.4 (6)	120.0 (7)
H(2)-C(7)-C(6)	121.1 (13)	
H(2)-C(7)-C(8)	119.4 (13)	
H(3)-C(8)-C(7)	119.1 (12)	
H(3)-C(8)-C(9)	120.7 (13)	
H(4)-C(9)-C(8)	119.5 (12)	
H(4)-C(9)-C(10)	120.3 (10)	
H(5)-C(10)-C(9)	119.1 (14)	
H(5)-C(10)-C(11)	121.1 (14)	
H(6)-C(11)-C(10)	119.5 (8)	
H(6)-C(11)-C(6)	120.1 (9)	
Around Second Phenyl Ring		
C(17)-C(12)-C(13)	118.6 (4)	119.1 (7)
C(12)-C(13)-C(14)	120.7 (4)	120.0 (7)
C(13)-C(14)-C(15)	119.3 (5)	120.5 (8)
C(14)-C(15)-C(16)	120.6 (5)	119.9 (9)
C(15)-C(16)-C(17)	119.5 (5)	120.8 (8)
C(16)-C(17)-C(12)	121.2 (4)	119.9 (8)
H(7)-C(13)-C(12)	121.1 (7)	
H(7)-C(13)-C(14)	118.2 (7)	
H(8)-C(14)-C(13)	118.2 (8)	
H(8)-C(14)-C(15)	122.6 (9)	
H(9)-C(15)-C(14)	119.9 (8)	
H(9)-C(15)-C(16)	119.4 (8)	
H(10)-C(16)-C(15)	120.7 (8)	
H(10)-C(16)-C(17)	119.8 (8)	
H(11)-C(17)-C(16)	120.0 (7)	
H(11)-C(17)-C(12)	118.8 (7)	
Around Third Phenyl Ring		
C(23)-C(18)-C(19)	120.1 (4)	120.6 (6)
C(18)-C(19)-C(20)	120.4 (6)	119.3 (7)
C(19)-C(20)-C(21)	119.6 (7)	120.0 (7)
C(20)-C(21)-C(22)	120.7 (5)	120.4 (7)
C(21)-C(22)-C(23)	120.5 (6)	120.6 (8)
C(22)-C(23)-C(18)	118.7 (7)	118.9 (7)
H(12)-C(19)-C(18)	118.9 (8)	
H(12)-C(19)-C(20)	120.6 (10)	
H(13)-C(20)-C(19)	120.7 (9)	
H(13)-C(20)-C(21)	119.8 (8)	
H(14)-C(21)-C(20)	120.7 (13)	
H(14)-C(21)-C(22)	118.5 (12)	
H(15)-C(22)-C(21)	122.2 (9)	
H(15)-C(22)-C(23)	117.3 (11)	
H(16)-C(23)-C(22)	120.7 (7)	
H(16)-C(23)-C(18)	120.6 (6)	

Footnotes to Table V

[a] The esd's given in parentheses for the internuclear separations and bond angles were calculated from the standard errors of the fractional coordinates for the corresponding atomic positions. [b] The esd's which are shown in parentheses for the average values are calculated from the formula $\sigma_{\bar{l}} = [\Sigma(\bar{l} - l_m)^2/(m^2 - m)]^{1/2}$, where m is the number of equivalent bonds, l_m is the length of the mth bond, and $\bar{l}$ is the mean length. [c] Although the precise location of the bridging H atom has not been resolved, the calculated bond angles which are given for the neutron and X-ray diffraction studies are based on the H atom located on the center of symmetry at $x = 0$, $y = 0$, and $z = 0$. The H–Cr–C bond angles are given to show the degree to which they vary from 90°.

Table VI. Structural Parameters (Bond Distances (Å) and Bond Angles (deg)) of the $[Cr_2(CO)_{10}(\mu\text{-H})]^-$ Monoanion

	$[Et_4N]^+$ salt	$[(Ph_3P)_2N]^+$ salt[a]	
	neutron	neutron	X-ray
	I. Cr–H–Cr Fragment		
Cr–Cr′	3.386 (6)	3.349 (13)	3.359 (2)
Cr–H	1.737 (19)	1.675	1.679
	1.707 (21)		
Cr–H–Cr′	158.9 (6)	180	180
H–Cr–C(1)	171.4 (4)	177.3 (5)	177.1
	II. Axial Carbonyl Group		
Cr(1)–C(1)	1.827 (3)	1.862 (8)	1.817 (8)
C(1)–O(1)	1.156 (3)	1.140 (7)	1.159 (7)
Cr–C(1)–O(1)	179.0 (2)	178.7 (7)	178.3 (7)
	III. Equatorial Carbonyl Groups		
Cr–C(2)	1.904 (3)	1.901 (10)	1.870 (8)
Cr–C(3)	1.890 (3)	1.895 (9)	1.886 (8)
Cr–C(4)	1.899 (3)	1.890 (10)	1.886 (8)
Cr–C(5)	1.897 (3)	1.899 (11)	1.880 (8)
av	1.898 (3)	1.896 (3)	1.881 (4)
C(2)–O(2)	1.139 (3)	1.133 (11)	1.136 (8)
C(3)–O(3)	1.136 (3)	1.144 (9)	1.138 (8)
C(4)–O(4)	1.137 (3)	1.141 (9)	1.138 (8)
C(5)–O(5)	1.136 (3)	1.139 (10)	1.134 (7)
av	1.137 (1)	1.139 (2)	1.137 (1)
Cr–C(2)–O(2)	177.6 (2)	178.2 (5)	177.8 (7)
Cr–C(3)–O(3)	177.0 (2)	176.9 (5)	176.5 (7)
Cr–C(4)–O(4)	177.7 (2)	177.7 (7)	178.2 (7)
Cr–C(5)–O(5)	177.2 (2)	179.0 (5)	177.2 (7)

[a] Structural parameters for the $[(Ph_3P)_2N]^+$ salt in this table are based upon a linear structure for the Cr–H–Cr bond.

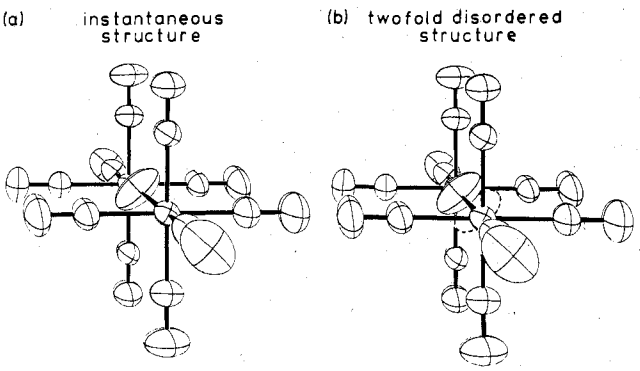

Figure 5. Molecular drawings of the $[Cr_2(CO)_{10}(\mu\text{-H})]^-$ monoanion for the $[Et_4N]^+$ salt depicting (a) the instantaneous C_{2v}-*2mm* structure and (b) the twofold disordered structure.

ternuclear distances of 1.707 (21) and 1.739 (19) Å. To minimize steric effects introduced by the nonlinearity (159°) of the Cr–H–Cr bond, the two centrosymmetrically related disordered sites for the hydrogen atom are situated such that the two coplanar Cr–H–Cr moieties are *staggered* with respect to the eclipsed array of equatorial carbonyl ligands. The resulting instantaneous C_{2v} configuration (Figure 5a), which is disordered to give the superimposed structure observed for the monoanion (Figure 5b), is favored sterically over an *eclipsed* arrangement since the latter would be susceptible to a twisting distortion of the two $Cr(CO)_5$ groups to an intermediate staggered structure for the equatorial carbonyls. In the $[(Ph_3P)_2N]^+$ salt the overall linear, eclipsed carbonyl configuration of approximate D_{4h} symmetry is maintained for the monoanion. Although bridging H atom's nuclear density maximum is centered between the two Cr atoms at a $\bar{1}$ site,

Table VII. Equations of "Best" Least-Squares Planes, Perpendicular Distances (Å) from These Planes, and Dihedral Angles between the Planes[a,b]

(A) Plane I through Cr, C(1), C(2), and C(4)
$-17.5594x + 9.2638y + 6.9759z - 0.0153 = 0$

Cr	0.013 (9)	H	−0.016
C(1)	−0.001 (6)	O(1)	−0.021 (9)
C(2)	−0.003 (6)	O(2)	−0.019 (11)
C(3)	1.907 (6)	O(3)	3.047 (10)
C(4)	−0.003 (6)	O(4)	−0.058 (9)
C(5)	−1.887 (7)	O(5)	−3.025 (9)

(B) Plane II through Cr, C(1), C(3), and C(5)
$12.5107x + 13.1238y - 7.5260z - 0.1546 = 0$

Cr	−0.046 (8)	H	−0.155
C(1)	−0.001 (6)	O(1)	0.051 (8)
C(2)	1.855 (6)	O(2)	2.987 (9)
C(3)	0.010 (6)	O(3)	0.103 (8)
C(4)	−1.936 (6)	O(4)	−3.075 (8)
C(5)	0.011 (6)	O(5)	0.054 (8)

(C) Plane III through Cr, C(2), C(3), C(4), and C(5)
$0.1035x - 2.89725y - 12.5517z + 1.6518 = 0$

Cr	−0.021 (7)	H	1.652
C(1)	−1.883 (5)	O(1)	−3.022 (7)
C(2)	0.012 (5)	O(2)	−0.003 (8)
C(3)	−0.007 (5)	O(3)	−0.014 (7)
C(4)	0.011 (5)	O(4)	0.033 (7)
C(5)	−0.007 (5)	O(5)	−0.015 (7)

(D) Plane IV through C(6), C(7), C(8), C(9), C(10), and C(11)
$-8.9146x - 6.7178y - 6.0600z + 7.3008 = 0$

C(6)	−0.001 (4)	H(2)	−0.010 (15)
C(7)	−0.002 (6)	H(3)	−0.018 (18)
C(8)	0.005 (7)	H(4)	−0.007 (16)
C(9)	−0.004 (7)	H(5)	0.029 (15)
C(10)	0.002 (6)	H(6)	0.028 (13)
C(11)	0.001 (5)	P	−0.074 (5)

(E) Plane V through C(12), C(13), C(14), C(15), C(16), and C(17)
$20.2400x + 3.0207y - 13.2871z - 8.2240 = 0$

C(12)	−0.007 (6)	H(7)	0.024 (15)
C(13)	0.003 (8)	H(8)	0.038 (23)
C(14)	0.014 (10)	H(9)	0.011 (22)
C(15)	−0.012 (11)	H(10)	0.006 (22)
C(16)	−0.007 (10)	H(11)	0.023 (18)
C(17)	0.013 (8)	P	−0.013 (6)

(F) Plane VI through C(18), C(19), C(20), C(21), C(22), and C(23)
$-2.7057x + 15.2071y - 3.0211z + 1.5007 = 0$

C(18)	0.002 (4)	H(12)	0.017 (12)
C(19)	−0.005 (5)	H(13)	0.010 (15)
C(20)	0.004 (6)	H(14)	−0.006 (12)
C(21)	0.002 (5)	H(15)	0.008 (14)
C(22)	−0.006 (5)	H(16)	0.030 (13)
C(23)	0.004 (5)	P	−0.032 (5)

Dihedral Angles (deg) between Planes

I and II	89.8	IV and V	76.5
I and III	89.8	IV and VI	86.8
II and III	88.9	V and VI	81.3

[a] The equations of the least-squares planes are expressed in terms of monoclinic fractional coordinates x, y, z. [b] The atomic positions used in the calculation of a given plane were weighted according to the errors in the fractional coordinates.

its highly anisotropic thermal ellipsoid (which is nearly cylindrical in shape with respect to the Cr–Cr line) is consistent with the instantaneous C_{2v} structure being disordered in equal populations among four possible equivalent sites rather than among the two sites as found in the $[Et_4N]^+$ salt.

Despite our inability in this case to distinguish a truly linear Cr–H–Cr geometry from such a composite of slightly bent structures, the outcome of recent low-temperature spectroscopic and structural studies on related systems strongly supports the latter representation. In an investigation of the general applicability of laser Raman spectroscopy for structural studies of metal–hydrogen–metal bonds in transition-metal hydrides, Shriver and co-workers[43,44] have performed low-temperature studies at 10 K on deuterated salts of the $[M_2(CO)_{10}(\mu\text{-H})]^-$ monoanion. Low temperatures are required since the stretching and bending modes associated with the central M–H–M unit are too weak to be observed at room temperature. From their work, a correlation between the frequency of the asymmetric stretching mode for the M–D–M group and the M–D–M bond angle was found. For an appreciably bent M–D–M bond, such as found in the $[W_2(CO)_{10}(\mu\text{-D})]^-$ monoanion of the $[(Ph_3P)_2N]^+$ salt, a significant decrease in the asymmetric stretching frequency is observed. However, for more nearly linear structures, such as found for the $[Cr_2(CO)_{10}(\mu\text{-D})]^-$ monoanion, a force field analysis shows that the vibrational frequency is rather insensitive to small bond angle deformations. Within the limitations of the solid-state Raman analysis, the analogous vibrational frequencies at 10 K of 1274 and 1270 cm^{-1} for the $[Et_4N]^+$ and $[(Ph_3P)_2N]^+$ salts, respectively, provide convincing evidence that the two salts possess a *similar* Cr–D–Cr structure at this temperature. This result, when extrapolated to room temperature, lends support to our conclusion that the observed thermal ellipsoid of the bridging hydrogen atom in the $[(Ph_3P)_2N]^+$ salt is due to a composite of disordered structures.

Additional structural evidence for the disordered, off-axis placement of the bridging hydrogen atom in the carbonyl-eclipsed configuration of the $[M_2(CO)_{10}(\mu\text{-H})]^-$ anion has been provided by Bau, Koetzle, and co-workers,[45] who have recently completed a neutron diffraction analysis of $[Et_4N]^+[W_2(CO)_{10}(\mu\text{-H})]^-$ at 14 K. In agreement with our neutron diffraction study[3] of $[Et_4N]^+[Cr_2(CO)_{10}(\mu\text{-H})]^-$, the bridging hydrogen atom is clearly displaced[46] from the metal–metal axis. The carbonyl-eclipsed structure, which is observed at room temperature, turns out at 14 K to be a disordered superposition of two bent, approximately eclipsed anions. A surprising aspect of their low-temperature study is the asymmetric disposition of the hydrogen atom which produces two widely different W–H distances of 1.718 (12) and 2.070 (12) Å. This result led Bau, Koetzle, and co-workers[45] to suggest that the $[W_2(CO)_{10}(\mu\text{-H})]^-$ anion may be described as a type of donor–acceptor complex, in which the electrons of the W–H bond in the 18-electron $[W(CO)_5H]^-$ species are donated to an empty orbital on the electron-deficient $W(CO)_5$ group.

On the basis of these spectroscopic and structural studies, the thermal ellipsoid of the bridging H atom in the $[(Ph_3P)_2N]^+$ salt represents a composite of equivalent, slightly bent Cr–H–Cr structures. The nature of this disorder can be better understood by a comparison of the relative sizes,[47] shapes, and orientations of the nuclear thermal ellipsoids of the bridging H atom and the axial carbonyl atoms in the $[Et_4N]^+$ and $[(Ph_3P)_2N]^+$ salts. In the former system the largest root-mean-square components of the thermal ellipsoids for the bridging hydrogen atom and each of the axial carbonyl atoms are directed approximately normal to the Cr–Cr axis. For the H atom the largest component of thermal displacement is perpendicular to the Cr–H–Cr plane, whereas for each of the axial carbonyl atoms it is nearly along the Cr–H–Cr plane. Although a corresponding twofold disorder of the one independent axial carbonyl group was not resolved at room temperature, the observed thermal anisotropy was rationalized[3,48] in terms of a composite of two half-carbon and two half-oxygen atoms each displaced ca. 0.08 Å and ca. 0.15 Å from their respective neutron-determined positions. These estimated displacements are considerably smaller than the observed ca. 0.3 Å displacements of the two disordered hydrogen sites from the midpoint of the Cr–Cr line and have led us to conclude that the overlap region of the Cr–H–Cr bond is located nearer to the centrosymmetric midpoint of the Cr–Cr line than to the half-weighted hydrogen atom positions. Consequently, the observed thermal anisotropy for the monoanion in the $[Et_4N]^+$ salt is consistent with the nonhydrogen structure representing the superposition of two slightly bent anions of C_{2v}-*mm*2 geometry. In comparison, the magnitudes of the corresponding thermal displacements (normal to the Cr–Cr line)[47] for the bridging H atom are significantly larger in the $[(Ph_3P)_2N]^+$ salt, whereas they are comparable in size for the corresponding axial carbonyl atoms. The thermal ellipsoid for the bridging H atom in the $[(Ph_3P)_2N]^+$ salt is sufficiently large to accommodate a composite of disordered sites with each displaced by ca. 0.2 Å from the "averaged" neutron determined position at the C_i-$\bar{1}$ site. For an unresolved twofold disorder of the bridging H atom, one would expect to observe an elongated ellipsoid with the maximum thermal displacement directed parallel to the plane which bisects opposite CO(eq)–Cr–CO(eq) bond angles. However, the pancake shape of the ellipsoid strongly favors a fourfold disorder. This hypothesis is in harmony with the distinctly different thermal anisotropy observed for the axial carbonyl atoms in the two salts. Rather than being directed along the Cr–H–Cr plane which bisects opposite OC(eq)–Cr–CO(eq) bond angles as was the case in the $[Et_4N]^+$ salt, the maximum and median thermal displacements for the axial carbonyl atoms in the $[(Ph_3P)_2N]^+$ salt are directed more nearly along the Cr–CO(eq) directions. Therefore, we suggest that the structural parameters associated with the bridging hydrogen atom represent a composite of a fourfold disorder of the off-axis hydrogen position.

The outcome of this neutron diffraction study of the bis(triphenylphosphine)iminium salt has shown the solid-state structure of the $[Cr_2(CO)_{10}(\mu\text{-H})]^-$ monoanion is affected to a much lesser degree than the tungsten analogue by its crystalline environment. A possible explanation for this difference is related to the degree of metal–metal overlap present in the M–H–M fragment of the two $[M_2(CO)_{10}(\mu\text{-H})]^-$ monoanions. Low-temperature neutron diffraction studies of $[(Ph_3P)_2N]^+[Cr_2(CO)_{10}(\mu\text{-H})]^-$ are underway in the hope of being able to resolve the level of disorder and to clarify our interpretation.

Acknowledgment. The support provided by the National Science Foundation under Grants CHE-77-22650 (to J.M.W.) and GP-19175X (to L.F.D.) for this research is gratefully acknowledged. Computer time for the refinement of the neutron data was provided to J.L.P. by the West Virginia Network for Educational Telecomputing. We would like to express our appreciation to Don Washecheck for his assistance in the analysis of the X-ray diffraction data and to Professor Robert Bau (University of Southern California) for communicating the results of the low-temperature neutron diffraction study of $[Et_4N]^+[W_2(CO)_{10}(\mu_2\text{-H})]^-$.

Registry No. $[(Ph_3P)_2N]^+[Cr_2(CO)_{10}(\mu\text{-H})]^-$, 62341-83-7.

Supplementary Material Available: A listing of the observed and calculated neutron diffraction and X-ray diffraction structure factors for $[(Ph_3P)_2N]^+[Cr_2(CO)_{10}(\mu\text{-H})]^-$ (21 pages). Ordering information

is given on any current masthead page.

References and Notes

(1) This work was performed under the auspices of the Division of Basic Energy Science of the Department of Energy.

(2) (a) West Virginia University. (b) Argonne National Laboratory. (c) University of Wisconsin—Madison.

(3) J. Roziere, J. M. Williams, R. P. Stewart, Jr., J. L. Petersen, and L. F. Dahl, *J. Am. Chem. Soc.*, **99**, 4497 (1977).

(4) (a) L. B. Handy, P. M. Treichel, L. F. Dahl, and R. G. Hayter, *J. Am. Chem. Soc.*, **88**, 366 (1966); (b) L. B. Handy, J. K. Ruff, and L. F. Dahl, *ibid.*, **92**, 7312 (1970).

(5) R. D. Wilson, S. A. Graham, and R. Bau, *J. Organomet. Chem.*, **91**, C49 (1975).

(6) R. G. Hayter, *J. Am. Chem. Soc.*, **88**, 366 (1966).

(7) TRACER II, lattice transformation and cell reduction program, S. L. Lawton, Mobil Research and Development Corp., Research Department, Paulsboro, N.J.

(8) The *Lp* factor for the monochromator on the Syntex $P\bar{1}$ diffractometer is given by the expression[9]

$$Lp = \frac{0.5}{\sin 2\theta}\left[\left(\frac{\cos^2 2\theta_M + \cos^2 2\theta}{1 + \cos^2 2\theta_M}\right) + \left(\frac{\cos 2\theta_M + \cos^2 2\theta}{1 + \cos 2\theta_M}\right)\right]$$

which assumes the graphite monochromator crystal is 50% mosaic and 50% perfect.

(9) R. A. Sparks, "Operations Manual Syntex $P\bar{1}$ Diffractometer", Syntex Analytical Instrument, Cupertino, Calif., 1970.

(10) J. C. Calabrese, FOBS, a Fortran diffractometer data reduction program, University of Wisconsin—Madison, 1972.

(11) J. C. Calabrese, SORTMERGE, Ph.D. Thesis (Appendix I), University of Wisconsin—Madison, 1971; a Fortran program for the merging and decay correction of X-ray data.

(12) J. F. Blount, DEAR, a Fortran absorption correction program based on the Busing-Levy method.[13]

(13) W. R. Busing and H. A. Levy, *Acta Crystallogr.*, **10**, 180 (1957).

(14) Linear mass absorption coefficient calculated from the "International Tables for X-Ray Crystallography", Vol. III, Kynoch Press, Birmingham, England, 1968, pp 157, 162.

(15) J. C. Calabrese, PHASE, Ph.D. Thesis (Appendix II), University of Wisconsin—Madison, 1971.

(16) J. C. Calabrese, MAP, a local Fortran Fourier summation and molecular assemblage program, 1972.

(17) J. C. Calabrese, "A Crystallographic Variable Matrix Least-Squares Refinement Program", University of Wisconsin—Madison, 1972.

(18) J. C. Calabrese, MIRAGE, Ph.D. Thesis (Appendix III), University of Wisconsin—Madison, 1971.

(19) The scattering factor tables used for all nonhydrogen atoms were those of Cromer and Mann[20] while the scattering factor table for the hydrogen atom was from Stewart et al.[21] The real and imaginary corrections for anomalous dispersion were $\Delta f' = 0.284$ and $\Delta f'' = 0.624$ for Cr and $\Delta f' = 0.090$ and $\Delta f'' = 0.095$ for P.[22]

(20) D. T. Cromer and J. B. Mann, *Acta Crystallogr., Sect. A*, **24**, 321 (1968).

(21) R. F. Stewart, E. R. Davidson, and W. T. Simpson, *J. Chem. Phys.*, **42**, 3175 (1965).

(22) D. T. Cromer and D. Liberman, *J. Chem. Phys.*, **53**, 1891 (1970).

(23) W. R. Busing, K. O. Martin, and H. A. Levy, "ORFLS, A Fortran Crystallographic Least-Squares Program", ORNL-TM-305, Oak Ridge National Laboratory, Oak Ridge Tenn., 1962.

(24) $R(F_o) = [\sum||F_o| - |F_c||/\sum|F_o|]$ and $R_w(F_o) = [\sum w_i||F_o| - |F_c||^2/\sum w_i|F_o|^2]^{1/2}$. All least-squares refinements of the X-ray data were based on the minimization of $\sum w_i||F_o| - |F_c||^2$ with individual weights $w_i = 1/\sigma^2(F_o)$.

(25) P. Day and J. Hines, *Oper. Systems Rev.*, **7**, 28 (1973).

(26) S. W. Peterson and H. A. Levy, *J. Chem. Phys.*, **20**, 704 (1952).

(27) $R(F_o^2) = \sum|F_o^2 - F_c^2|/\sum F_o^2$ and $R_w(F_o^2) = [\sum w_i|F_o^2 - F_c^2|^2/\sum w_i F_o^4]^{1/2}$. All least-squares refinements of the neutron data were based on the minimization of $\sum w_i|F_o^2 - S^2F_c^2|^2$ with individual weights $w_i = 1/\sigma^2(F_o^2)$. The neutron scattering amplitudes used[28] in this study were $b_{Cr} = 0.352$, $b_N = 0.940$, $b_P = 0.510$, $b_C = 0.663$, $b_O = 0.575$, and $b_H = -0.372$ (all units in 10^{-12} cm).

(28) G. E. Bacon, *Acta Crystallogr., Sect. A*, **28**, 357 (1972).

(29) For a listing of the observed and calculated structure factors, see description of supplementary material at the end of the paper.

(30) The computer programs which were used in performing the necessary calculations for the neutron data with their accession names in the World List of Crystallographic Computer Programs (3rd ed) are as follows: data reduction and absorption correction, DATALIB; data averaging and sort, DATASORT; Fourier summation, CNTFOR, modification of FORDAP; direct methods analysis, MULTAN; least-squares refinement, ORXFLS3; error analysis of distances and angles, ORFEE3; and structural drawings, ORTEP II. For the determination of the least-squares planes the program PLNJO was used.[31]

(31) J.-O. Lundgren, University of Uppsala, Uppsala, Sweden; based on the method of D. Blow, *Acta Crystallogr.*, **13**, 168 (1960).

(32) S. C. Abrahams and E. T. Keve, *Acta Crystallogr.*, **23**, 971 (1967).

(33) The half-normal probability plot was obtained from a recent version of the program NORMPLOT, written by G. Christoph.

(34) "International Tables for X-Ray Crystallography", Vol. IV., Kynoch Press, Birmingham, England, 1974.

(35) The P–N–P bond angle falls in the range 134.6–141.8° for the bis(triphenylphosphine)iminium salts of $[M_2(CO)_{10}]^{2-}$ (M = Mo, W)[4b] $[Cr_2(CO)_{10}I]^-$,[36] $[M_2Ni_3(CO)_{10}]^{2-}$ (M = Mo, W),[37] $[HFe(CO)_4]^-$,[38] $[Fe(CO)_4CN]^-$,[39] $[Fe_2(CO)_8]^{2-}$,[40] $[FeCo(CO)_8]^-$,[40] $[Co(CO)_4]^-$,[41] and $[HW_2(CO)_{10}]^-$.[5]

(36) L. B. Handy, J. K. Ruff, and L. F. Dahl, *J. Am. Chem. Soc.*, **92**, 7327 (1970).

(37) J. K. Ruff, R. P. White, and L. F. Dahl, *J. Am. Chem. Soc.*, **93**, 2159 (1971).

(38) M. B. Smith and R. Bau, *J. Am. Chem. Soc.*, **95**, 2388 (1973).

(39) S. A. Goldfield and K. N. Raymond, *Inorg. Chem.*, **13**, 770 (1974).

(40) H. B. Chin, M. B. Smith, R. D. Wilson, and R. Bau, *J. Am. Chem. Soc.*, **96**, 5285 (1974).

(41) J. Chiang, M.S. Thesis, University of Southern California, 1974.

(42) R. D. Wilson and R. Bau, *J. Am. Chem. Soc.*, **96**, 7601 (1974).

(43) Presented in part at the Second Joint CIC–ACS Meeting at the Symposium on Transition Metal Hydride Chemistry, Montreal, Canada, June 1977.

(44) D. Shriver, C. B. Cooper III, and S. Onaka, *Adv. Chem. Ser.*, **No. 167**, 232 (1978).

(45) (a) D. W. Hart, R. Bau, and T. F. Koetzle, submitted for publication; (b) R. Bau, R. G. Teller, S. W. Kirtley, and T. F. Koetzle, *Acc. Chem. Res.*, in press.

(46) The off-axis displacement for the bridging hydrogen atom is 0.71 (1) Å in $[Et_4N]^+[W_2(CO)_{10}(\mu_2\text{-H})]^-$ as compared to ca. 0.3 Å in $[Et_4N]^+[Cr_2(CO)_{10}(\mu\text{-H})]^-$.

(47) The corresponding median and maximum root-mean-square thermal displacements for H, C(1), and O(1) atoms of the anion in the $[Et_4N]^+$ salt are $\mu(2) = 0.262$ (20) and $\mu(3) = 0.441$ (11) Å, $\mu(2) = 0.224$ (2) and $\mu(3) = 0.287$ (3) Å, and $\mu(2) = 0.305$ (3) and $\mu(3) = 0.391$ (4) Å, respectively.

(48) J. L. Petersen, L. F. Dahl, and J. M. Williams, *Adv. Chem. Ser.*, **No. 167**, 11 (1978).